Vol. 25, No. 2, pp. 243-264 (2025)
Journal of Agricultural Physics
ISSN 0973-032X
https://doi.org/10.56093/JAP.v25i2.14

Research Article

Influence of Weather Variability on Intercepted Photosynthetically Active Radiation and Yield of Wheat

ARAVIND K.S.[1], ANANTA VASHISTH[1*], CHANDRAKANT RAJ H.[1], P. KRISHNAN[1], MONIKA KUNDU[1], SHIV PRASAD[2] AND M.C. MEENA[3]

[1]Division of Agricultural Physics, [2]Division of Environment Science, [3]Division of Soil Science and Agricultural Chemistry, ICAR-Indian Agricultural Research Institute, New Delhi-110012

ABSTRACT

Sowing time plays a critical role in regulating wheat productivity in the Indo-Gangetic Plains, where weather variability and terminal heat stress frequently constrain crop growth and yield. A field experiment was conducted during two Rabi seasons (2020–21 and 2021–22) at the research farm of ICAR–Indian Agricultural Research Institute, New Delhi, to evaluate the influence of sowing date on wheat phenology, canopy development, radiation interception, biomass accumulation and grain yield. Three wheat varieties (HD 3086, HD 2967 and PBW 723) were sown under timely, late and very late sowing conditions in a split-plot design. Periodic measurements of key biophysical variables, including leaf area index (LAI), intercepted photosynthetically active radiation (IPAR), fractional interception of PAR (fIPAR) and above-ground biomass, were recorded at major phenological stages, and grain yield was measured at harvest. Timely sowing resulted in superior canopy development, characterized by higher peak LAI (≈4.3–4.6), near-complete radiation interception (fIPAR 0.93–0.96) and greater cumulative IPAR (~700–750 MJ m^{-2}), leading to maximum biomass accumulation. Delayed sowing compressed phenological duration, reduced peak LAI by 20–25%, constrained fIPAR (0.86–0.90 under late and 0.72–0.78 under very late sowing), and decreased cumulative IPAR by 20–35%, resulting in 25–35% reductions in biomass. These canopy- and radiation-mediated effects translated into grain yield penalties of 6–10% under late sowing and 22–29% under very late sowing across the two seasons. Among the cultivars, HD 3086 consistently maintained higher canopy persistence, radiation interception and yield stability under delayed sowing. The close correspondence between phenology-specific canopy traits, radiation interception and grain yield underscores the central role of canopy-mediated radiation capture in determining wheat productivity. Timely sowing, coupled with genotypes exhibiting stable canopy function, emerges as a robust strategy for sustaining wheat yield under increasing thermal stress in the Indo-Gangetic Plains.

Key words: Leaf area index, Intercepted photosynthetically active radiation, Biomass, Wheat yield

Introduction

Wheat (*Triticum aestivum* L.) productivity is fundamentally controlled by the interaction of weather variability, crop phenology and canopy structural dynamics, which together regulate radiation interception, biomass accumulation and yield realization. Variations in temperature and solar radiation influence the rate and duration of phenological phases, thereby shaping leaf area development and the temporal dynamics of intercepted photosynthetically active radiation (PAR). The radiation-based framework of crop

*Corresponding author,
Email: ananta.iari@gmail.com

growth emphasizes that seasonal biomass production is primarily determined by cumulative intercepted PAR, modulated by canopy architecture and prevailing environmental conditions (Monteith, 1977; Sinclair & Muchow, 1999). Within this framework, sowing date is a key management factor, as it defines the thermal and radiative environment experienced by the crop and strongly influences leaf area index (LAI), intercepted PAR (IPAR), fraction of intercepted PAR (fIPAR), biomass accumulation and final grain yield (Pradhan *et al*., 2018; Zhao *et al*., 2017).

Variation in sowing time alters wheat phenology by modifying the duration and sequencing of vegetative and reproductive stages. Timely sowing generally prolongs vegetative growth under favourable temperature and radiation regimes, promoting greater canopy expansion and higher cumulative IPAR, whereas delayed sowing compresses thermal time accumulation, accelerates phenological development and constrains leaf area formation (Pathania *et al*., 2019). These phenology-driven changes in canopy structure directly affect radiation interception and biomass production over the growing season (Borrelli *et al*., 2011; Mubvuma *et al*., 2020). Consequently, IPAR and fIPAR serve as integrative biophysical indicators linking canopy status to growth potential and yield outcomes (Sandana *et al*, 2012).

Empirical studies across diverse agro-ecological regions corroborate these relationships. In the semi-arid Indo-Gangetic Plains, timely sowing consistently results in higher seasonal IPAR and fIPAR, greater biomass accumulation and superior grain yield compared with late sowing, which often exposes reproductive stages to supra-optimal temperatures and reduces the effective duration of radiation capture (Aggarwal & Mall, 2002; Pradhan *et al*., 2018; Dubey *et al*., 2020). Similar sowing date effects have been reported in the North China Plain, where early sowing enhanced canopy development and cumulative IPAR under variable climatic conditions (Sun *et al*., 2013), and in Mediterranean environments, where delayed sowing reduced LAI and intercepted radiation due to accelerated phenology and heat stress during reproductive stages (Sandaña & Calderini, 2012). These findings collectively demonstrate that sowing date modulates how weather variability is translated into canopy radiation interception and growth responses.

From a biophysical perspective, fIPAR is closely linked to LAI and canopy vertical structure, which determine the efficiency of radiation capture within the canopy (Norman & Welles, 1983; Stoll & Schmid, 1998). Increasing LAI generally enhances fIPAR and cumulative IPAR, provided that canopy architecture permits efficient light penetration and limits self-shading (Monsi & Saeki, 2005; Chen *et al*., 2017). Weather variability further modulates these processes by influencing both incident PAR availability and phenological progression. Elevated temperatures and altered radiation regimes can shorten the effective period of radiation interception by accelerating senescence and truncating reproductive development, thereby limiting biomass accumulation even when early-season canopy development is favourable (Asseng *et al*., 2015; Aslam *et al*., 2025). Interannual variability in solar radiation and temperature therefore contributes substantially to fluctuations in IPAR, biomass production and yield (Borrelli *et al*., 2011; Vashisth *et al*., 2022).

Under Indian conditions, particularly in the semi-arid subtropical environment of northern India, these interactions are especially pronounced. Field experiments at the Indian Agricultural Research Institute (IARI), New Delhi, have shown that delayed sowing leads to significant reductions in LAI, IPAR and biomass accumulation, resulting in yield penalties relative to crops sown within the optimum window (Joshi & Singh, 2019; Aravind *et al*., 2022). Such responses reflect the broader agro-climatic constraints of the Indo-Gangetic Plains, where increasing temperature variability and frequent terminal heat events interact with sowing schedules to constrain canopy development and the duration of effective radiation interception.

Despite extensive documentation of sowing date effects, important gaps remain in the quantitative understanding of how weather variability interacts with phenology to regulate canopy radiation interception and biomass dynamics. Many studies rely on aggregate correlations between LAI or phenological timing and final yield, providing limited insight into stage-specific sensitivities of IPAR and fIPAR to weather drivers or the temporal robustness of these relationships across seasons and cultivars. In particular, relatively few investigations have explicitly examined phenology-specific patterns of radiation interception and their contribution to biomass accumulation under contrasting sowing dates for modern wheat genotypes.

Accordingly, the present study, conducted at the ICAR–IARI experimental fields in New Delhi, aims to: (i) quantify the phenology-specific influence of weather variability on canopy radiation interception (IPAR, fIPAR) and leaf area development under different sowing dates; (ii) assess stage-wise responses of above-ground biomass accumulation to weather conditions for three widely cultivated wheat varieties (HD 3086, HD 2967 and PBW 723); and (iii) evaluate the temporal consistency and transferability of phenology-based canopy–biomass relationships across seasons. By integrating detailed phenological observations with high-frequency measurements of canopy radiation interception and robust statistical analysis, this study seeks to provide a mechanistically grounded understanding of how sowing time mediates the effects of weather variability on canopy development and biomass production in wheat, with implications for adaptive management in the Indo-Gangetic Plains.

Materials and Methods

Experimental site and climate

Field experiments were conducted during the *Rabi* seasons of 2020–21 and 2021–22 at the research farm of the Division of Agricultural Physics, ICAR–Indian Agricultural Research Institute (ICAR-IARI), New Delhi, India (28°38′23″ N, 77°09′27″ E; 228.6 m AMSL). The site has a uniform, level topography and deep, well-drained sandy loam soil. The region experiences a subtropical semi-arid climate, with hot summers, cool winters, and a long-term mean annual rainfall of ~710 mm, predominantly received during July–September.

Experimental Design and Crop Management

The experiment was laid out in a split-plot design with three replications, comprising three sowing dates as main plots and three wheat cultivars—HD 3086, HD 2967 and PBW 723—as sub-plots. Sowing was carried out under timely, late, and very late conditions each year: 19 Nov, 4 Dec, and 19 Dec (2020–21); 10 Nov, 25 Nov, and 10 Dec (2021–22). Plots measured 5.0 m × 3.5 m, with a seed rate of 100 kg ha^{-1}, row spacing of 22.5 cm, and sowing depth of 4 cm. Flood irrigation (5 cm) was applied at critical growth stages. Fertilizers were applied at 120:60:40 kg ha^{-1} (N: P: K), with full P and K and 50% N as basal, and remaining N top-dressed after initial irrigations.

Meteorological Observations

Daily weather data (maximum and minimum temperature, relative humidity, rainfall and bright sunshine hours) were obtained from the Agro-meteorological Observatory, ICAR-IARI, New Delhi, for the entire crop growth period.

Crop Phenology

Crop phenological stages were recorded for all treatments, covering germination, tillering, jointing–booting, flowering, grain filling and physiological maturity. Crop duration ranged from 120 to 150 days, depending on cultivar and sowing date. HD 3086 and HD 2967 are medium-duration cultivars, while PBW 723 is early maturing and relatively better adapted to delayed sowing.

Leaf Area Index

Leaf area index (LAI) was measured at 10-day intervals from tillering to grain filling using an LAI-2000 Plant Canopy Analyzer (LI-COR, USA). Measurements consisted of four below-canopy and one above-canopy readings, with mean values used for analysis.

Radiation Interception

Photosynthetically active radiation (PAR) above and below the canopy was measured weekly using a LI-191SA line quantum sensor (LI-COR Inc., USA) between 11:30 and 12:30 h IST on clear days. Intercepted PAR (IPAR) and fraction of intercepted PAR (fIPAR) were computed as:

IPAR= I0 – TC

fIPAR = IPAR/ I0

I0 = Radiation received at the top of the canopy

TC = Transmitted radiation to soil through the canopy

R0 = Reflected radiation from the top of the canopy

RC = Reflected radiation from soil

Biomass and Yield

Above-ground biomass was determined by oven-drying five randomly sampled plants per plot at 65 °C for 48 h and expressed on a gm^{-2} basis. Thousand-grain weight was measured using a precision electronic balance. Grain yield was estimated after sun-drying, threshing and weighing, and expressed as gm^{-2}.

Results and Discussion

Weather Conditions during the Wheat Growing Season (Rabi 2020–21)

Weather conditions during the wheat growing season (SMW 45–17) exhibited pronounced intra-seasonal variability relative to long-term normals (Fig. 1 a & b). Observed bright sunshine hours were generally lower than normal during early crop establishment, particularly around SMW 1–2, followed by a steady increase during the reproductive and grain-filling phases. Wind speed showed a progressive seasonal rise, with observed values closely tracking normal trends but exceeding long-term means during late-season weeks (SMW 11–17). Pan evaporation remained low during early vegetative growth and increased markedly from mid-season onward, surpassing normal values during the reproductive phase. Overall, the season was characterized by reduced radiation availability during early growth and enhanced atmospheric demand during later stages, providing contrasting weather conditions for evaluating sowing date–dependent crop responses.

Weather Conditions during the Wheat Growing Season (Rabi 2021–22)

During the wheat growing season of *Rabi* 2021–22 (SMW 45–17), weekly mean maximum and minimum temperatures showed a clear seasonal pattern (Fig. 2 a & b). Both maximum and minimum temperatures declined from sowing until mid-winter, with minimum temperatures reaching their lowest

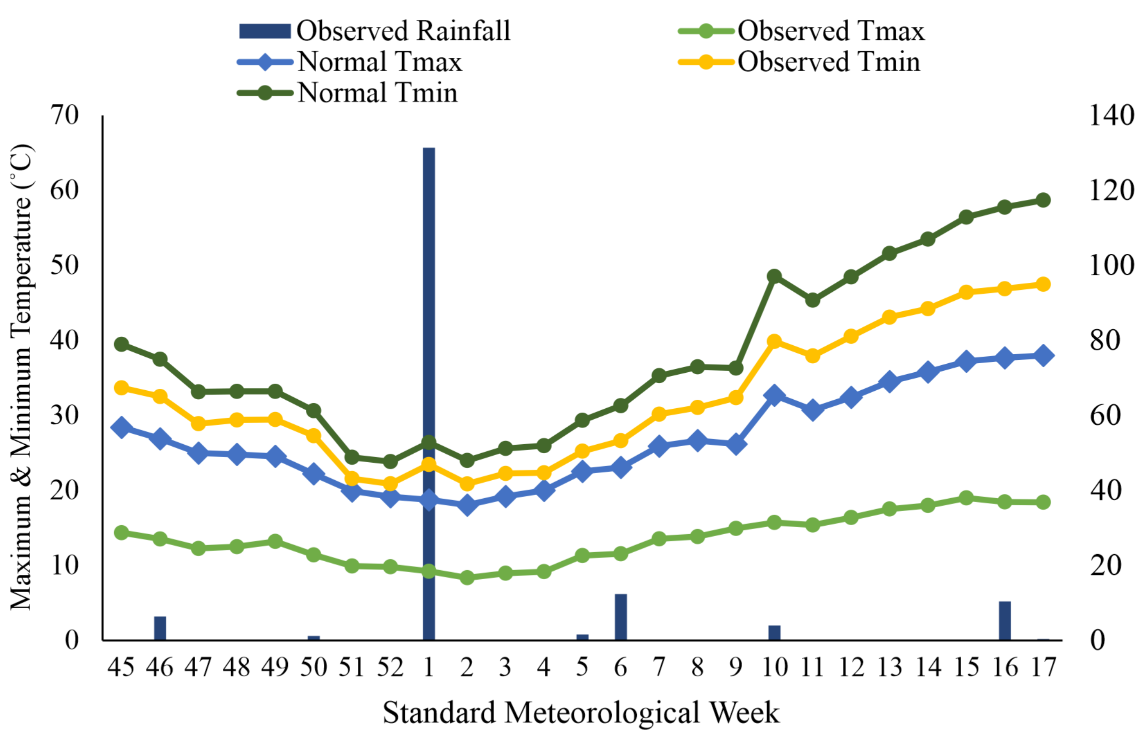

Fig. 1a. Weekly mean maximum and minimum temperatures and cumulative rainfall during wheat growing period *Rabi* 2020-2021 at ICAR-IARI, New Delhi

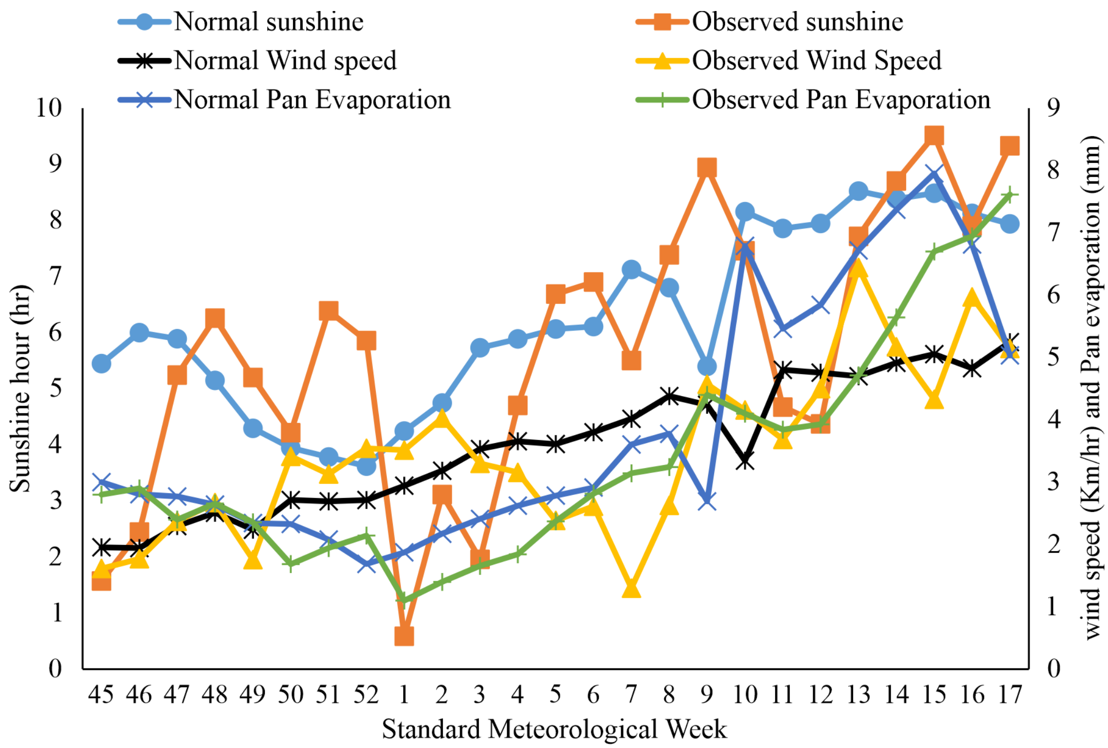

Fig. 1b. Weekly mean maximum and minimum temperatures and cumulative rainfall during wheat growing period *Rabi* 2020-2021 at ICAR-IARI, New Delhi

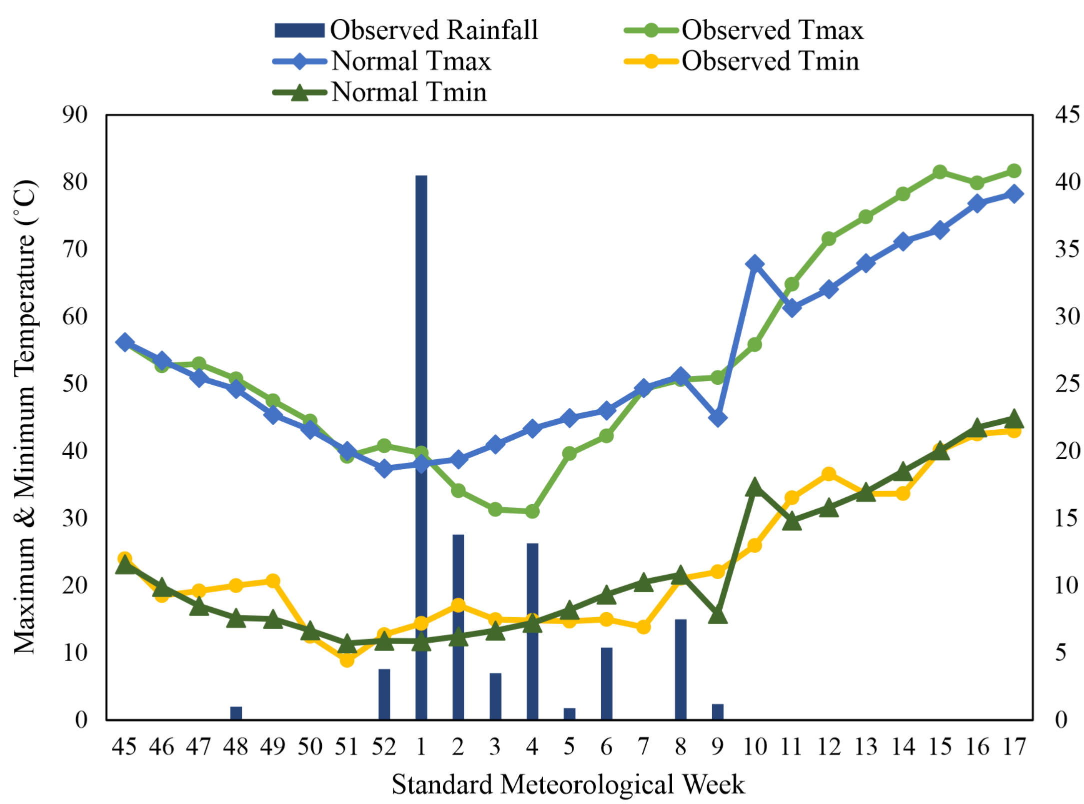

Fig. 2a. Weekly mean maximum and minimum temperatures and cumulative rainfall during wheat growing period *Rabi* 2021-2022 at ICAR-IARI, New Delhi

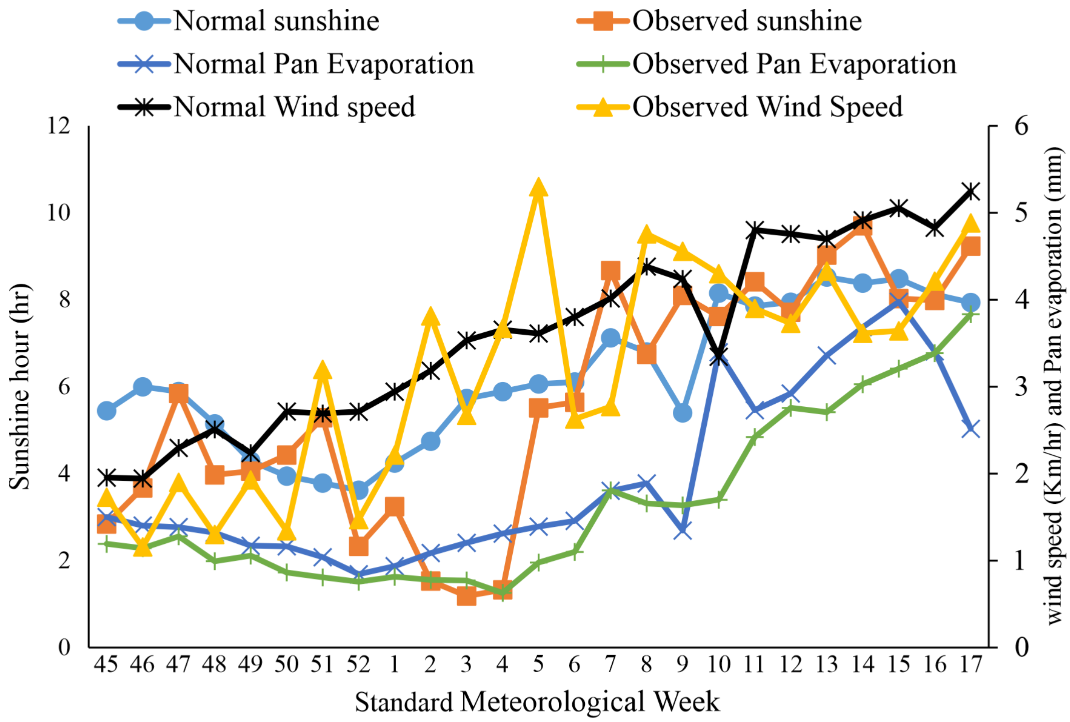

Fig. 2b. Weekly mean sunshine hours, wind speed and pan evaporation during wheat growing period *Rabi* 2021-2022 at ICAR-IARI, New Delhi

levels during SMW 1–2, followed by a progressive rise toward the reproductive and grain-filling stages. Maximum temperatures increased sharply from SMW 10 onward, coinciding with anthesis and grain filling. Rainfall during the season was low and episodic, with isolated events concentrated mainly during the early to mid-vegetative phase and negligible precipitation during the later stages. The combination of rising temperatures and limited rainfall during reproductive growth indicates heightened thermal stress, particularly affecting late- and very late-sown wheat.

Temporal Dynamics of Leaf Area Index (LAI) during Rabi 2020–21

Leaf area index (LAI) exhibited a clear temporal pattern across sowing dates and cultivars during Rabi 2020–21, characterized by a gradual increase during vegetative growth, a peak near anthesis, and a subsequent decline with the onset of senescence (Fig. 3a). Sowing date strongly influenced both the magnitude and persistence of canopy development. With timely sowing, peak LAI reached 4.28, 4.62, and 4.56 for PBW-723, HD-2967, and HD-3086, respectively. Delayed sowing progressively reduced peak LAI to 3.97, 4.18, and 4.04 under late sowing, and further to 3.30, 3.52, and 3.64 under very late sowing.

The timing of maximum LAI advanced with sowing delay, occurring around 90 DAS under timely and late sowing but shifting to approximately 80 DAS under very late sowing, indicating accelerated phenological development under higher thermal regimes. The reduction in peak LAI from timely to very late sowing ranged from 20.2% (HD-3086) to 23.8% (HD-2967). Although HD-2967 exhibited marginally higher LAI under timely and late sowing, HD-3086 maintained the highest LAI under very late sowing, exceeding PBW-723 and HD-2967 by 10.3% and 3.4%, respectively.

Temporal Dynamics of Leaf Area Index (LAI) during Rabi 2021–22

Leaf area index (LAI) dynamics during Rabi 2021–22 exhibited a characteristic seasonal pattern across sowing dates and cultivars, with progressive canopy expansion during vegetative growth, attainment of maximum LAI near flowering, and a

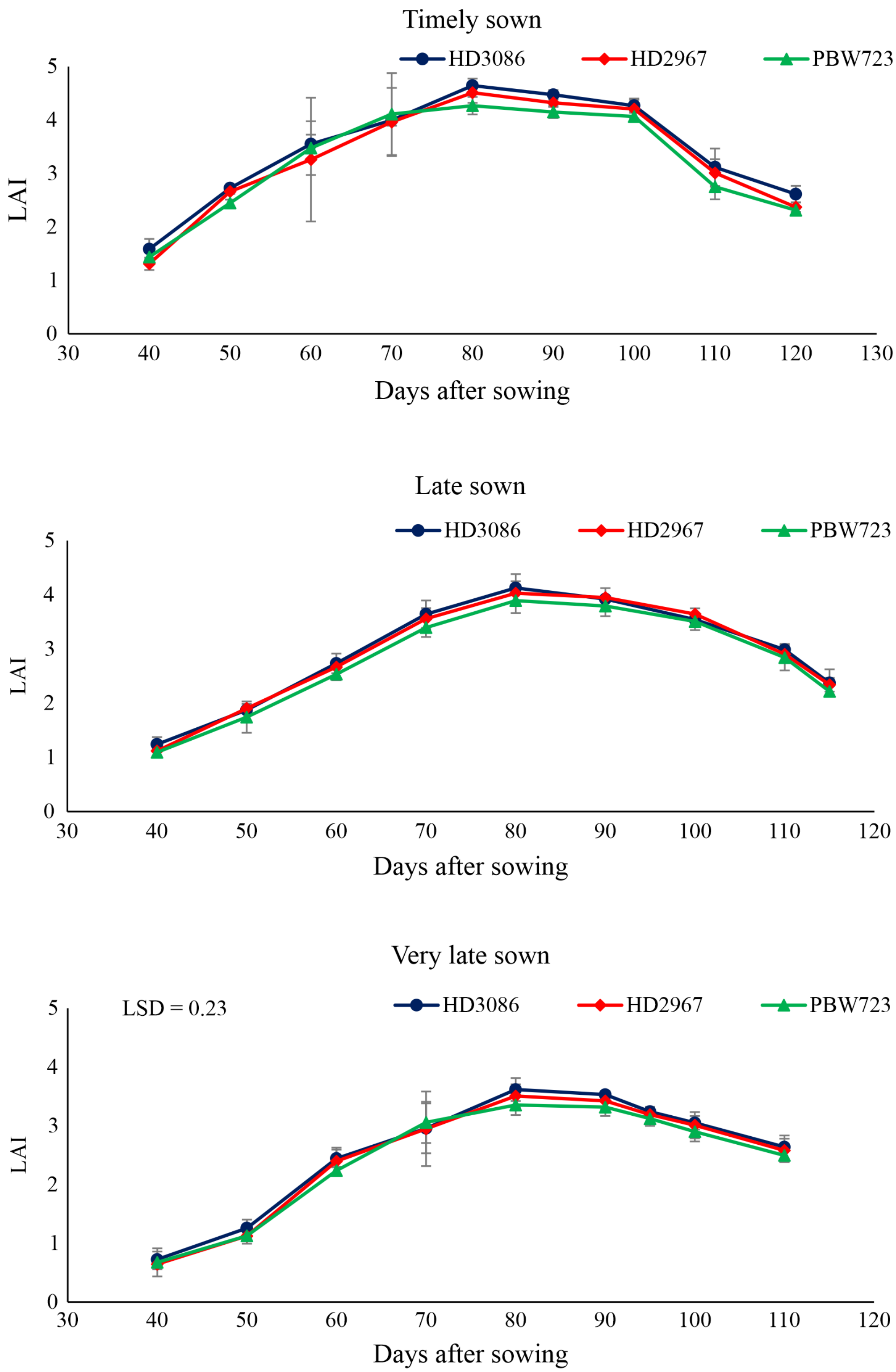

Fig. 3a. Temporal dynamics of leaf area index (LAI) of wheat under different sowing dates during Rabi 2020–21

gradual decline thereafter (Fig. 3b). Timely sown wheat consistently achieved the highest canopy development, while late and very late sowings resulted in progressively reduced LAI. Peak LAI values under timely sowing were 4.02, 4.31 and 4.46 for PBW-723, HD-2967 and HD-3086, respectively, declining to 3.80, 3.92 and 4.03 under late sowing and further to 3.13, 3.20 and 3.44 under very late sowing. Maximum LAI occurred around 90 DAS under timely and late sowings but shifted earlier to approximately 80 DAS under very late sowing, indicating accelerated phenological progression under elevated thermal regimes.

The reduction in peak LAI from timely to very late sowing averaged 22.1% (PBW-723), 25.8% (HD-2967) and 22.8% (HD-3086). Across sowing environments, HD-3086 consistently maintained the highest LAI, exceeding PBW-723 by 8.3–9.9% and HD-2967 by 2.8–3.7%, reflecting superior canopy stability under both optimal and thermally stressed conditions.

Temporal Growth Dynamics and Biomass Accumulation during Rabi 2020–21

Total above-ground biomass of wheat increased progressively from early vegetative growth to the reproductive phase, reaching maximum values between 110 and 120 DAS, after which accumulation approached a plateau, indicating the onset of physiological maturity (Fig. 4a). Across all cultivars, timely sowing resulted in the highest biomass accumulation throughout the growth period, whereas late and very late sowings showed progressively reduced biomass due to shortened growth duration and increased terminal heat exposure.

Under timely sowing, biomass ranged from 15–1610 g m^{-2} (PBW-723), 18–1610 g m^{-2} (HD-3086) and 12–1580 g m^{-2} (HD-2967). These ranges contracted under late sowing to 10–1360, 12–1330 and 9–1350 g m^{-2}, respectively, and further under very late sowing to 7–1170, 8–1190 and 8–1170 g m^{-2}. Relative to timely sowing, total biomass under very late conditions declined by 27–29% in PBW-723, 26–28% in HD-2967, and 25–27% in HD-3086, corresponding to mean reductions of 27.3%, 27.0% and 26.4%, respectively. Among genotypes, HD-3086 consistently maintained the highest biomass and the smallest proportional decline under delayed sowing, whereas PBW-723 exhibited the greatest sensitivity.

Temporal Growth Dynamics and Biomass Accumulation during Rabi 2021–22

Total above-ground biomass during Rabi 2021–22 followed a progressive accumulation pattern across sowing dates and cultivars, increasing from early vegetative growth and reaching maximum values between 110 and 120 DAS, after which accumulation approached a plateau indicative of physiological maturity (Fig. 4b). Biomass magnitudes were consistently highest under timely sowing, while late and very late sowings showed successive reductions, reflecting shortened crop duration and enhanced terminal heat stress.

Under timely sowing, biomass ranged from 18–1620 g m^{-2} (PBW-723), 20–1620 g m^{-2} (HD-3086) and 18–1580 g m^{-2} (HD-2967). These ranges declined under late sowing to 15–1240, 18–1330 and 16–1280 g m^{-2}, respectively, and further under very late sowing to 12–940, 15–1120 and 13–1080 g m^{-2}. Relative to timely sowing, biomass declined by approximately 15–18% under late sowing and 30–35% under very late sowing. PBW-723 exhibited the greatest reduction, whereas HD-3086 consistently maintained the highest biomass across sowing environments.

Intercepted Photosynthetically Active Radiation (IPAR) during Rabi 2020–21

Intercepted photosynthetically active radiation (IPAR) during Rabi 2020–21 increased progressively from early vegetative growth to the reproductive phase, reaching maximum values around 100-110 DAS, followed by a gradual decline with canopy senescence (Fig. 5a). Sowing time significantly influenced both the magnitude and duration of radiation interception. Timely sowing resulted in the highest cumulative IPAR due to favourable thermal conditions and prolonged canopy persistence, whereas late and very late sowings exhibited progressively lower IPAR because of shortened vegetative duration and accelerated senescence under elevated terminal temperatures.

Under timely sowing, IPAR increased from approximately 180–250 MJ m^{-2} at 40 DAS to 700–

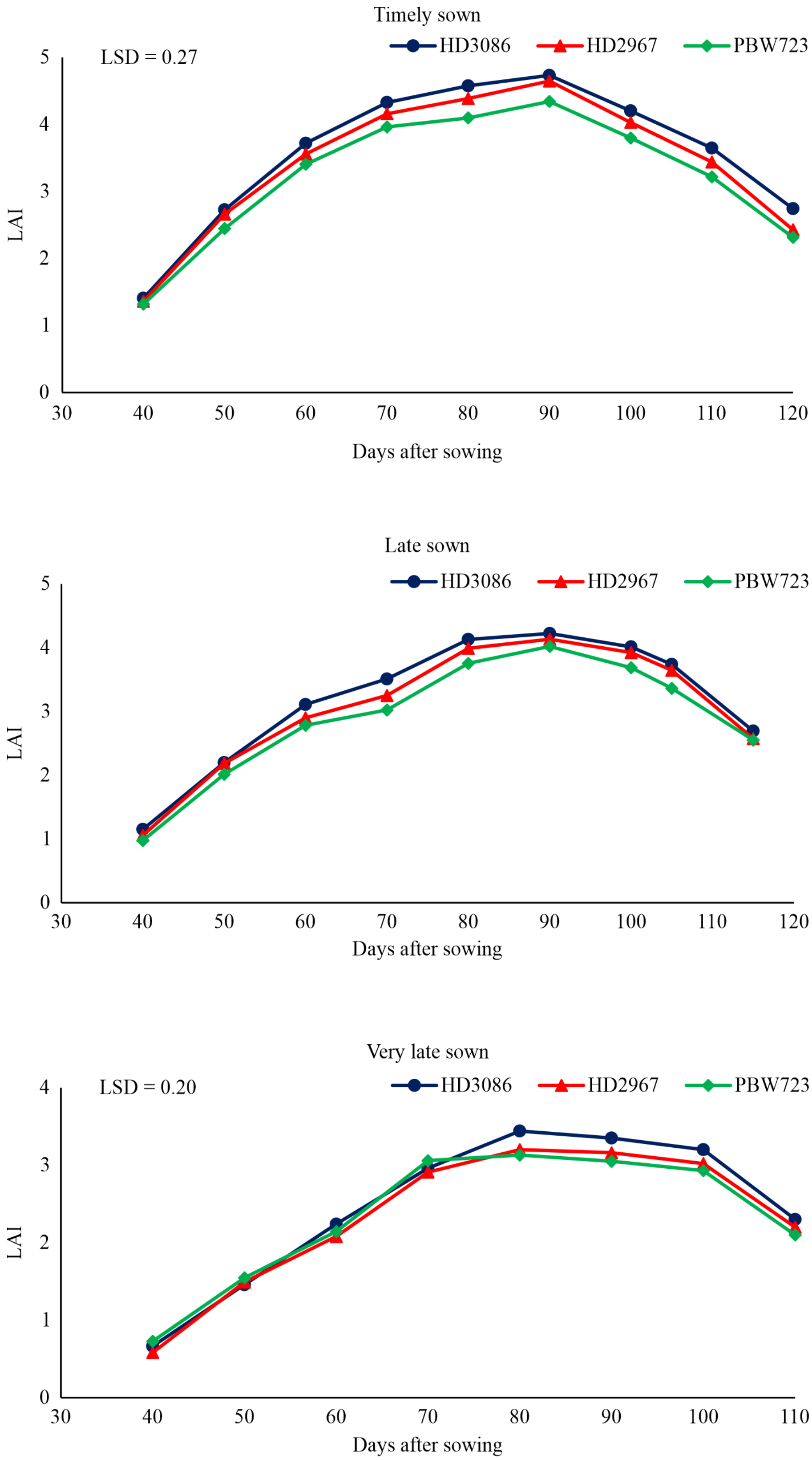

Fig. 3b. Temporal Dynamics of Leaf Area Index (LAI) of Wheat Under Different Sowing Dates During *Rabi* 2021–22

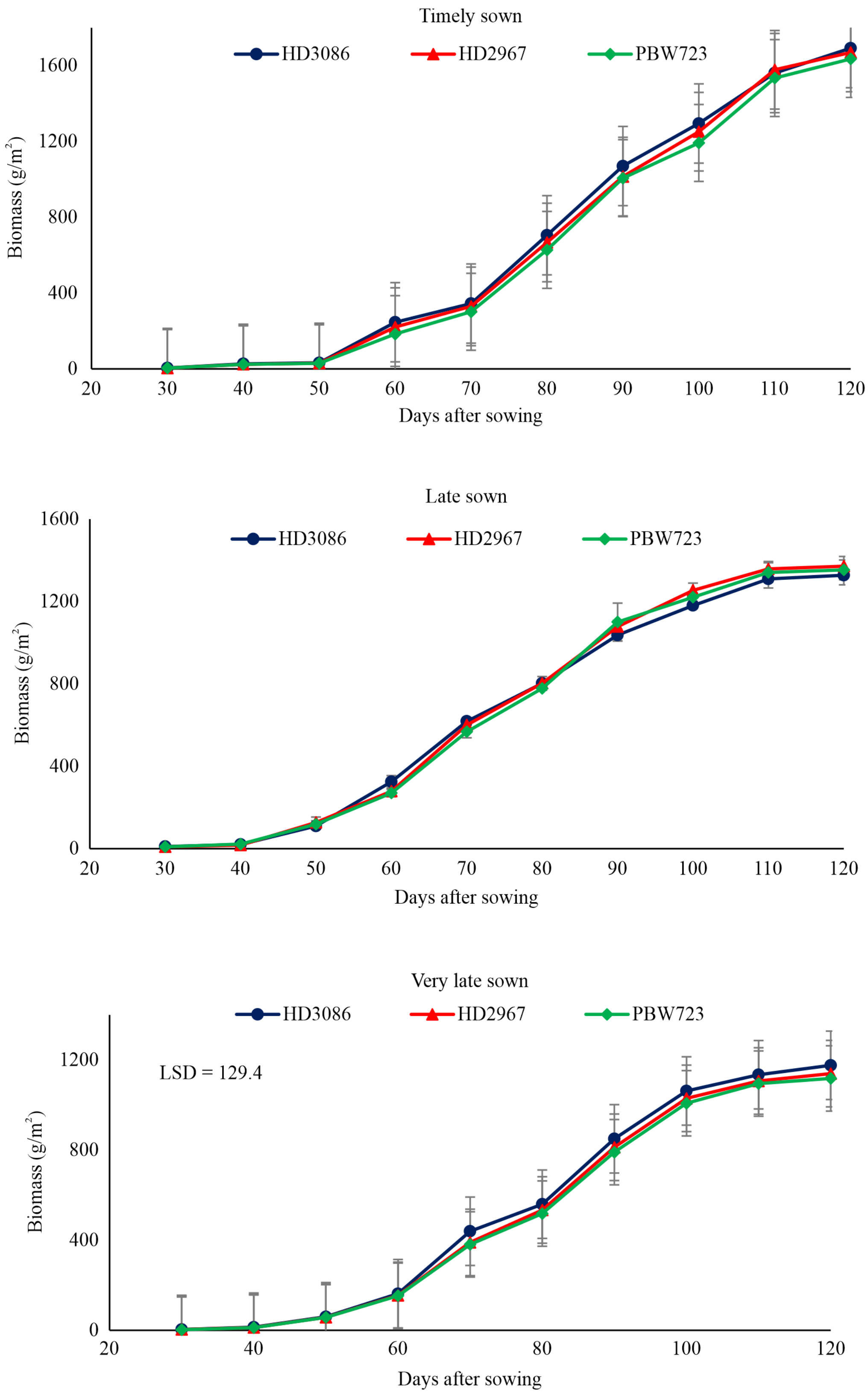

Fig. 4a. Temporal growth dynamics and biomass accumulation in wheat under different sowing dates during *Rabi* 2020–21

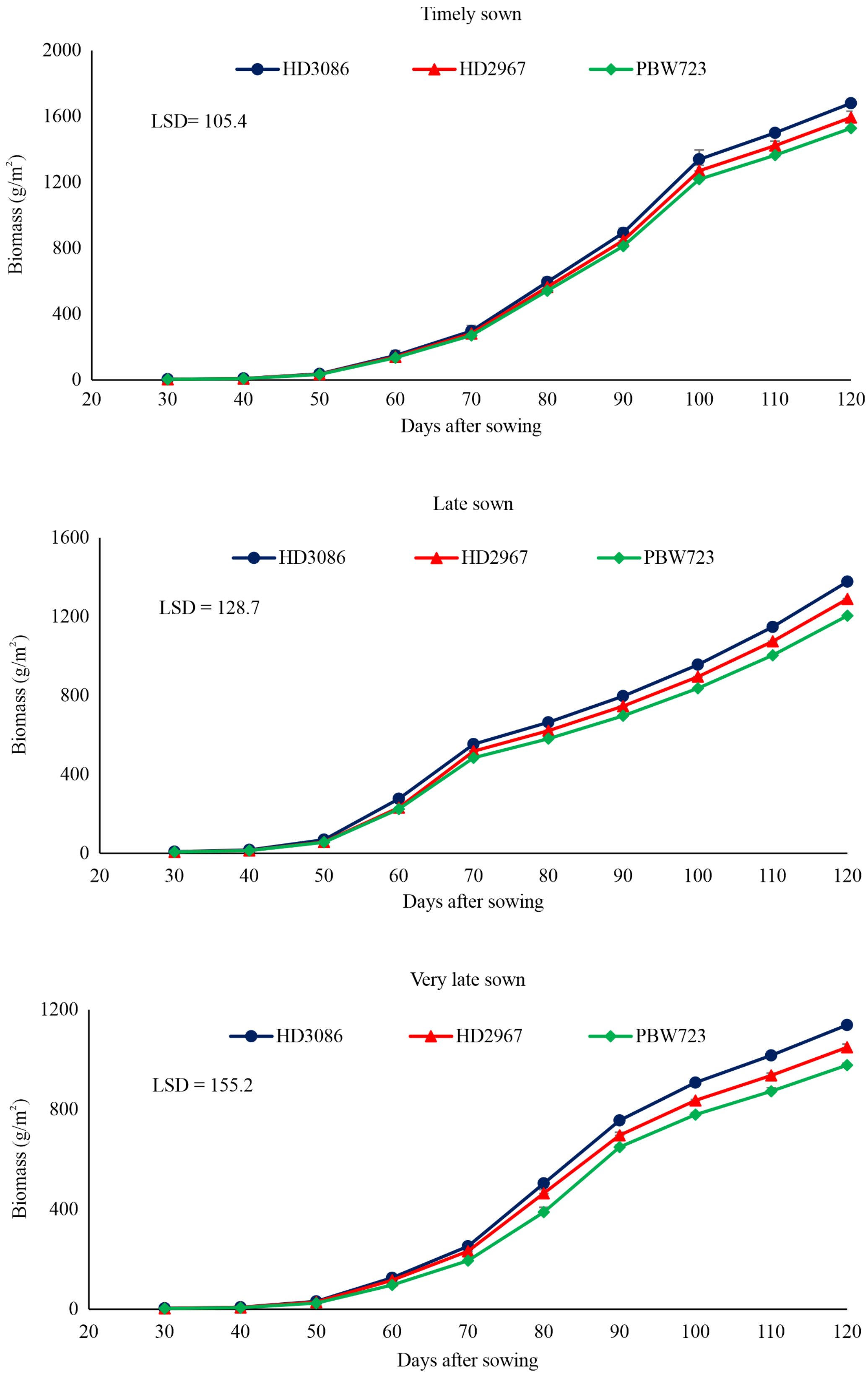

Fig. 4b. Temporal growth dynamics and biomass accumulation in wheat under different sowing dates during *Rabi* 2021–22

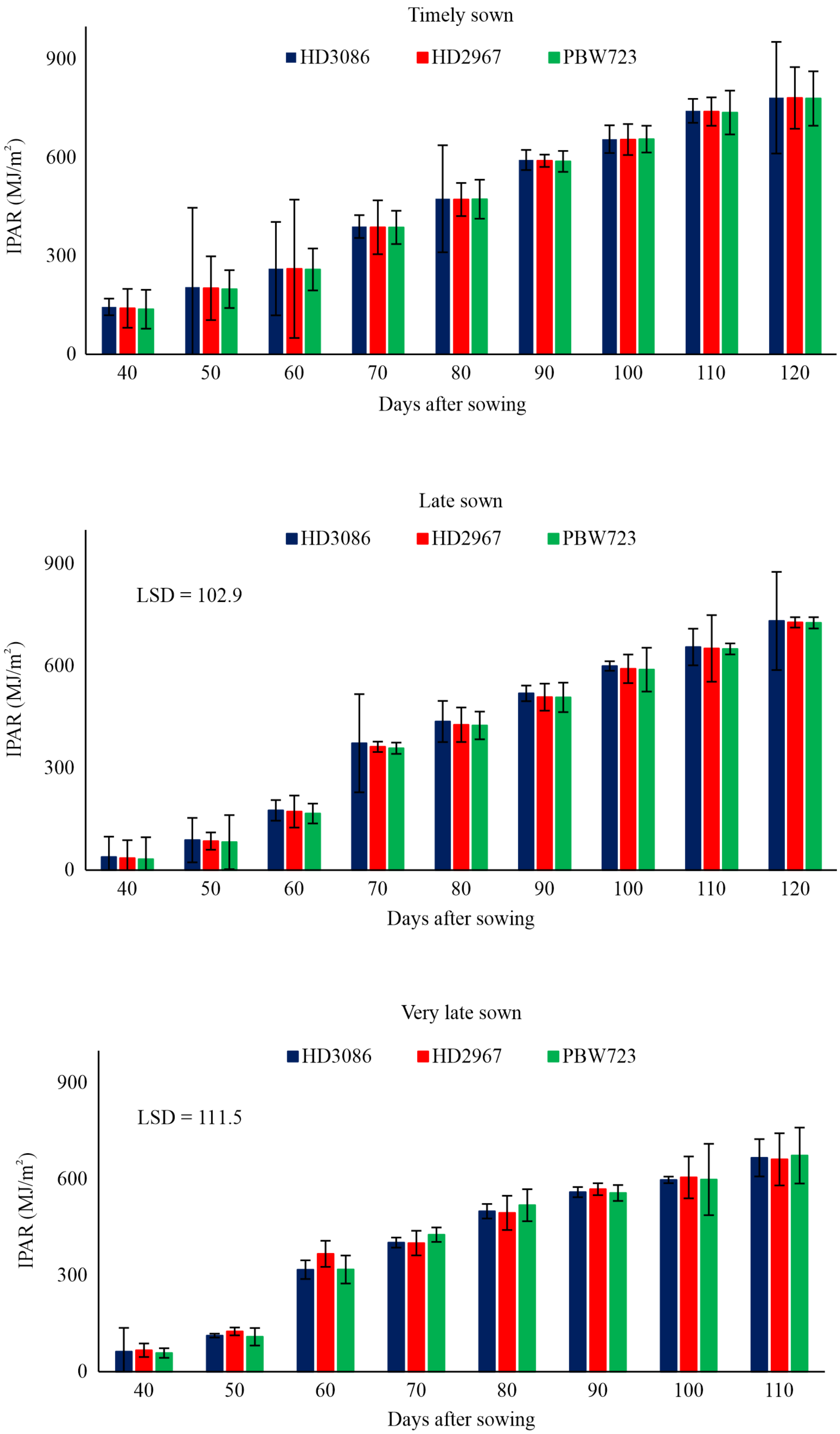

Fig. 5a. Impact of sowing time and variety on intercepted photosynthetically active radiation (IPAR) during *Rabi* 2020–21

750 MJ m^{-2} by 120 DAS. Corresponding values declined to about 90–690 MJ m^{-2} under late sowing and further to 110–630 MJ m^{-2} under very late sowing, representing average reductions of 20–25% and 30–35%, respectively, relative to timely sowing. Across all sowing environments, HD-3086 consistently recorded the highest IPAR, followed by HD-2967, while PBW-723 exhibited comparatively lower interception throughout the growth period.

Intercepted Photosynthetically Active Radiation (IPAR) during Rabi 2021–22

During Rabi 2021–22, intercepted photosynthetically active radiation (IPAR) exhibited a seasonal progression comparable to the previous year, although overall magnitudes were marginally lower across all sowing environments (Fig. 5b). IPAR increased steadily from early vegetative stages through canopy expansion, reaching maximum values between 110 and 120 DAS, followed by a gradual decline as senescence progressed and green leaf area diminished.

Timely sown wheat consistently intercepted the greatest amount of radiation, with IPAR increasing from approximately 180–260 MJ m^{-2} at 40 DAS to peak values of 650–720 MJ m^{-2}. In contrast, maximum IPAR declined to 560–610 MJ m^{-2} under late sowing and further to 470–530 MJ m^{-2} under very late sowing, representing average reductions of 20–25% and 30–35%, respectively, relative to timely sowing. Across all sowing dates, HD-3086 maintained higher IPAR throughout the growth period, followed by HD-2967, whereas PBW-723 consistently intercepted lower radiation. Radiation use efficiency and relative leaf water content had significantly higher values, while leaf water potential had lower values in the timely sown crop, followed by the late and very late sown crops. Yield was higher in HD-3086, followed by HD-2967 and PBW-723, across all weather conditions. Canopy air temperature difference had a positive value in a very late sown crop, particularly during flowering and grain-filling stages. This reflects in the yield. Yield was more in the timely sown crop as compared to the late and very late sown crop (Vashisth *et al.*, 2022).

Fractional Interception of Photosynthetically Active Radiation (fIPAR) during Rabi 2020–21

The seasonal dynamics of fractional interception of photosynthetically active radiation (fIPAR) during Rabi 2020–21 exhibited a characteristic progression across sowing dates and cultivars (Fig. 6a). fIPAR increased from low values during early vegetative growth, rose sharply with canopy expansion, and declined gradually with the onset of senescence. Under timely sowing, fIPAR increased from approximately 0.25–0.30 at 40 DAS to peak values close to 0.94–0.96 by 80–90 DAS, followed by a decline to about 0.78–0.80 at maturity.

Sowing time markedly influenced both the magnitude and duration of interception. Late sowing attained a comparable but shorter peak (≈0.91–0.93), whereas very late sowing showed substantially constrained interception, with maximum fIPAR limited to 0.75–0.78 and a rapid decline thereafter. By maturity, fIPAR values decreased to approximately 0.78 (timely), 0.82 (late) and 0.74 (very late), reflecting progressive shortening of the effective photosynthetic period with sowing delay. Across environments, HD-3086 consistently maintained marginally higher fIPAR, followed by HD-2967 and PBW-723.

Fractional Interception of Photosynthetically Active Radiation (fIPAR) during Rabi 2021–22

During Rabi 2021–22, fractional interception of photosynthetically active radiation (fIPAR) followed a seasonal trajectory similar to the previous year, though with marginally lower magnitudes across sowing environments (Fig. 6b). fIPAR increased steadily from early vegetative stages, peaked during canopy closure, and declined thereafter as senescence progressed. Under timely sowing, fIPAR increased from approximately 0.28–0.30 at 40 DAS to peak values of 0.93–0.96 at 80–90 DAS, followed by a gradual decline to 0.78–0.82 by maturity.

Delayed sowing markedly constrained interception dynamics. Late sowing attained lower peak fIPAR values (0.86–0.90), while very late sowing exhibited substantially reduced maxima

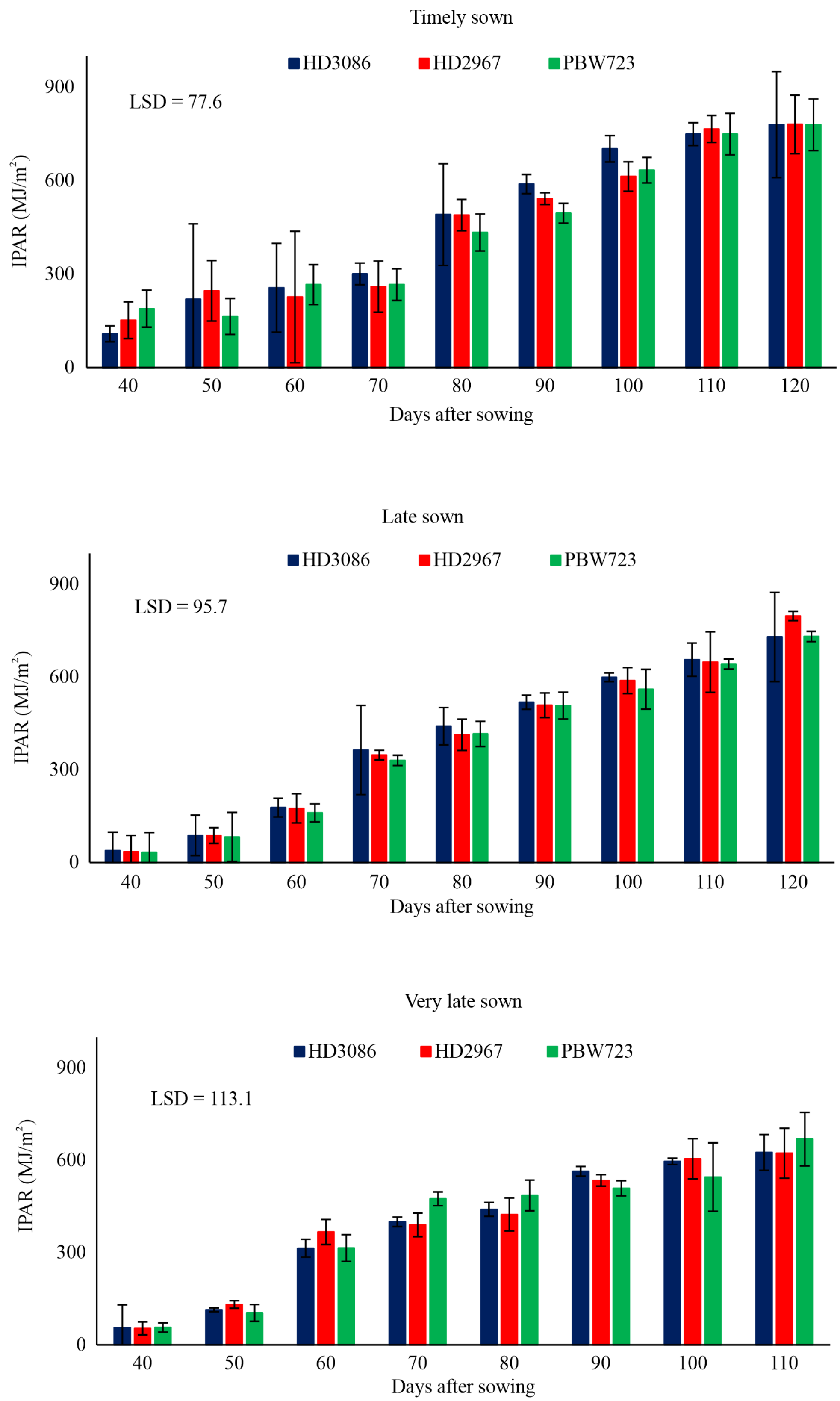

Fig. 5b. Impact of sowing time and variety on intercepted photosynthetically active radiation (IPAR) during *Rabi* 2021–22

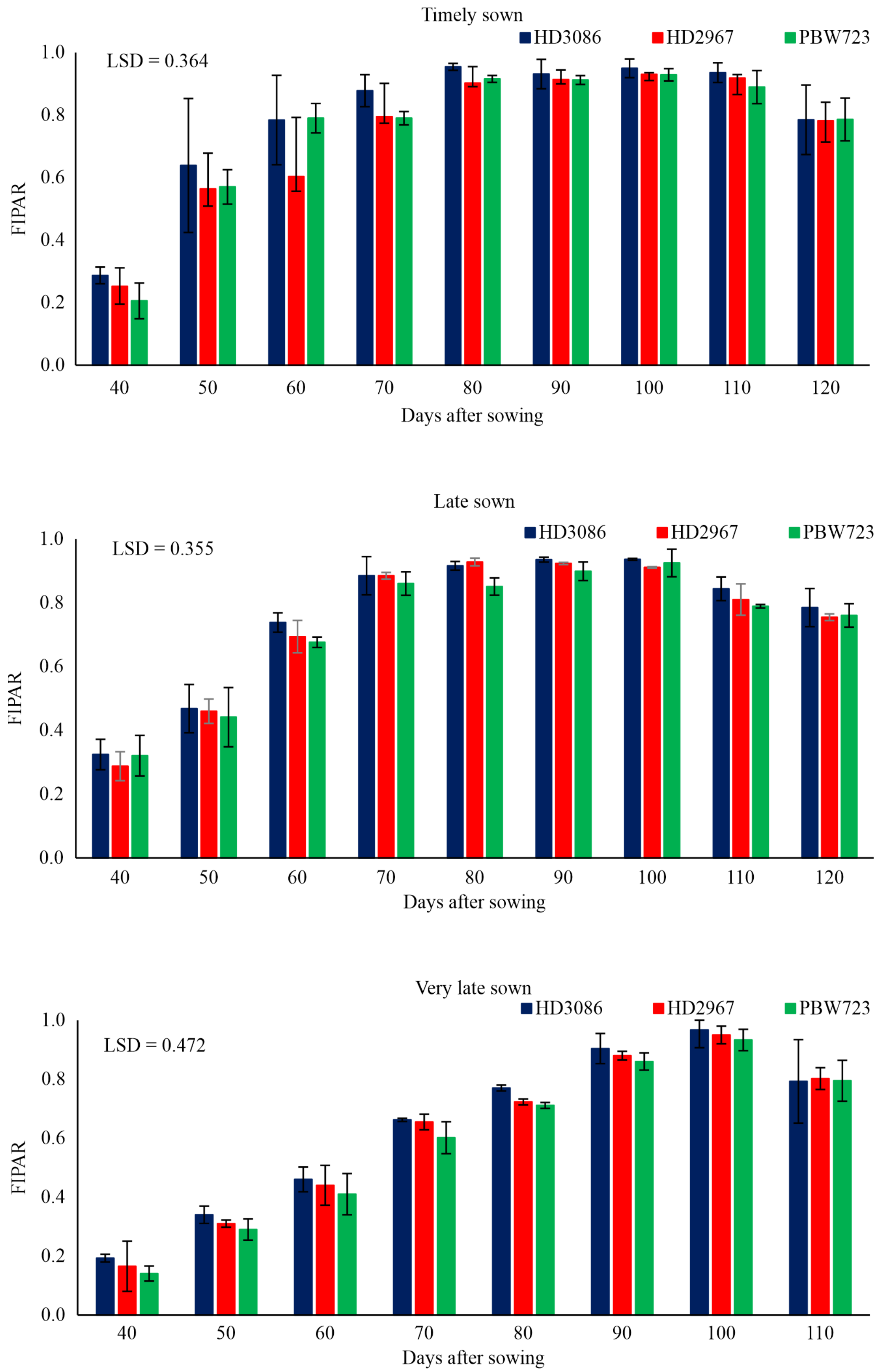

Fig. 6a. Influence of sowing time on fractional interception of photosynthetically active radiation (FIPAR) in wheat during *Rabi* 2020–21

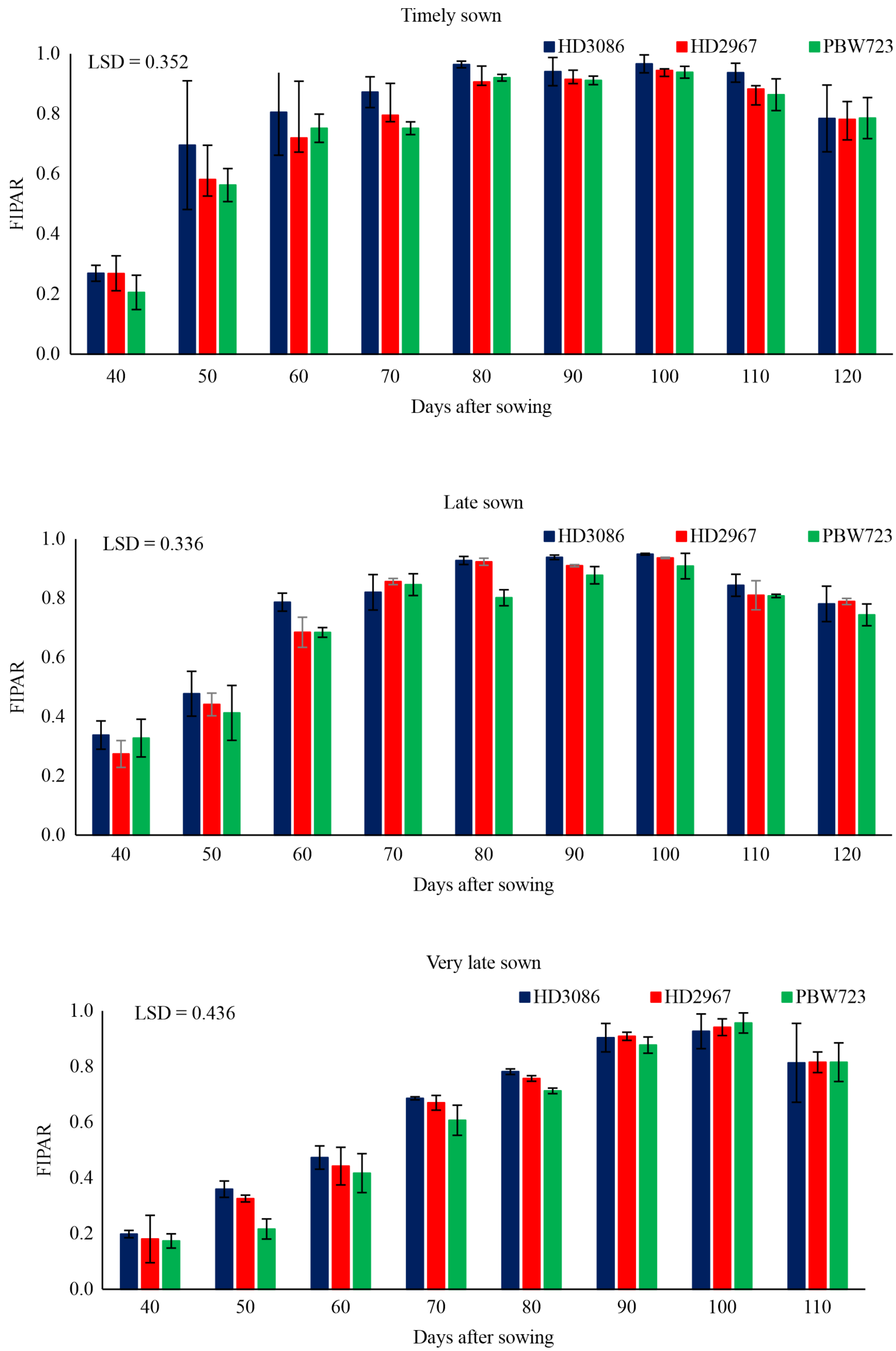

Fig. 6b. Influence of sowing time on fractional interception of photosynthetically active radiation (FIPAR) in wheat during *Rabi* 2021–22

(0.72–0.78), corresponding to mean reductions of approximately 22–30% and 35–40%, respectively, relative to timely sowing. Across all sowing environments, HD-3086 consistently recorded the highest fIPAR, followed by HD-2967 and PBW-723, reflecting superior canopy persistence and delayed senescence under thermal stress.

Across seasons and sowing environments, LAI-driven canopy development exerted primary control over radiation interception and subsequent biomass accumulation, as reflected in coordinated variations in IPAR and fIPAR. Timely sowing produced higher peak LAI (≈4.3–4.6), enabling near-complete canopy closure and elevated peak fIPAR values of 0.93–0.96, which sustained cumulative IPAR of ~700–750 MJ m^{-2} and supported maximum biomass production. In contrast, delayed sowing reduced peak LAI by 20–25%, thereby compressing canopy duration and restricting maximum fIPAR to 0.86–0.90 (late) and 0.72–0.78 (very late), resulting in corresponding IPAR reductions of ~20–25% and ~30–35%, respectively. This shortening of the effective radiation interception window translated directly into biomass reductions of ~25–35% under late and very late sowing, despite comparable incident PAR. Genotypic differences in interception efficiency closely followed canopy stability; HD-3086, which consistently maintained higher LAI under thermal stress, achieved marginally higher fIPAR and IPAR and consequently sustained higher biomass across sowing dates. These treatment effects were statistically supported by LSD• .• … values of 0.33–0.47 for fIPAR and 94–113 MJ m^{-2} for IPAR, confirming that phenology-mediated LAI dynamics mechanistically regulate radiation capture and biomass formation under variable sowing environments.

Grain Yield Response to Sowing Time and Variety across **Rabi** *2020–21 and 2021–22*

Grain yield across Rabi 2020–21 and 2021–22 declined systematically with delayed sowing for all wheat varieties, closely reflecting concurrent reductions in LAI, intercepted radiation (IPAR and fIPAR), and total biomass accumulation. Under timely sowing, grain yield ranged from 4750–5220 kg ha^{-1} in 2020–21 and 4300–4750 kg ha^{-1} in 2021–22, with HD 3086 consistently recording the highest yield, followed by HD 2967 and PBW 723. Shifting sowing to the second window resulted in modest yield reductions of 6–8% in 2020–21 and 7–10% in 2021–22, corresponding to moderate declines in peak LAI and cumulative IPAR.

In contrast, very late sowing caused substantial yield penalties, with reductions of 26–29% in 2020–21 and 22–24% in 2021–22 relative to timely sowing, as yields declined to 3400–3850 kg ha^{-1} and 3360–3650 kg ha^{-1}, respectively. These pronounced losses aligned with 20–25% reductions in peak LAI, 30–35% decreases in IPAR, lower fIPAR (0.72–0.78), and 25–35% reductions in biomass, indicating a shortened effective assimilatory period under terminal heat stress. Across both seasons and sowing environments, HD 3086 exhibited superior yield stability, consistent with its greater canopy persistence, higher radiation interception, and sustained biomass production. Collectively, the results confirm that phenology-mediated canopy development and radiation capture are the dominant biophysical drivers of yield variation under contrasting sowing environments. Crop growth and seed yield were relatively higher in the first sown wheat crop varieties because of more congenial weather conditions during the entire crop growth period. Radiation use efficiency was found to be higher in first sown crop as compared to late sown crop. Delay in sowing time reduces the yield significantly. From this study it was concluded that crop micro environment changed due to different sowing dates, strongly influences different phenological stages and crop yield. Seed yield therefore could be optimized by doing appropriate management practices during different phenological stages for obtaining favorable microclimatic conditions for crop growth (Vashisth *et al.,* 2020, Vashisth *et al.,* 2012).

High-temperature stress during the grain-filling periods significantly decreased the grain yield. Reduction in the grain yield was associated with a reduction in starch and amylose content in the grains. The protein content in the grains is less affected by terminal heat stress. Cultivar HD-3086 had higher growth, yield as well as quality parameters, compared to HD-2967 and PBW-723 in all treatments, hence could be adopted by farmers in northwest India (Roy *et al.,* 2024).

Table 1. Variation in grain yield (kg ha^{-1}) of wheat varieties under timely, late and very late sowing conditions during Rabi seasons 2020–21 and 2021–22

Variety	Date of sowing	Grain yield
PBW 723	First Date of sowing (19 November 2020)	4750
	Second Date of sowing (4 December 2020)	4360
	Third Date of sowing (19 December 2020)	3400
HD 3086	First Date of sowing (19 November 2020)	5220
	Second Date of sowing (4 December 2020)	4890
	Third Date of sowing (19 December 2020)	3850
HD 2967	First Date of sowing (19 November 2020)	4940
	Second Date of sowing (4 December 2020)	4590
	Third Date of sowing (19 December 2020)	3550
PBW 723	First Date of sowing (10 November 2021)	4300
	Second Date of sowing (25 November 2021)	3950
	Third Date of sowing (10 December 2021)	3360
HD 3086	First Date of sowing (10 November 2021)	4750
	Second Date of sowing (25 November 2021)	4420
	Third Date of sowing (10 December 2021)	3650
HD 2967	First Date of sowing (10 November 2021)	4560
	Second Date of sowing (25 November 2021)	4100
	Third Date of sowing (10 December 2021)	3490

The present study provides a mechanistic, radiation-based interpretation of how sowing time modulates wheat growth, biomass accumulation and grain yield through its influence on phenology, canopy development and radiation interception under the semi-arid subtropical conditions of the Indo-Gangetic Plains (IGP). Across seasons, sowing date emerged as the dominant driver of variability in leaf area index (LAI), intercepted photosynthetically active radiation (IPAR), fractional interception of PAR (fIPAR), biomass production and yield, highlighting the central role of phenology-mediated canopy dynamics in determining wheat productivity.

Sowing time, phenology and canopy development

Delayed sowing consistently reduced peak LAI and shortened the duration of effective canopy cover, reflecting accelerated phenological development under elevated thermal regimes. This response aligns with earlier findings that temperature governs the rate of leaf appearance, tillering duration and canopy expansion in wheat (Slafer & Rawson, 1994; Porter & Gawith, 1999; Pathania *et al*., 2019). The observed advancement of maximum LAI from ~90 DAS under timely sowing to ~80 DAS under very late sowing corroborates reports from the IGP and other warm wheat-growing regions, where thermal time accumulation accelerates developmental transitions and curtails vegetative growth under delayed planting (Aggarwal & Mall, 2002; Asseng *et al*., 2015). Similar reductions in LAI with sowing delay have been reported in wheat grown in the North China Plain and Mediterranean environments, where compressed phenology limits leaf expansion and hastens senescence (Sandaña & Calderini, 2012; Martínez *et al*., 2019; Sun *et al*., 2013).

Radiation interception as a function of LAI and canopy persistence

Consistent with radiation-use theory (Monteith, 1977; Sinclair & Muchow, 1999), reductions in LAI translated directly into lower fIPAR and cumulative IPAR under delayed sowing. Timely sown wheat achieved near-complete canopy closure (fIPAR H”0.93–0.96), sustaining high radiation interception over a longer period, whereas late and very late sowings exhibited progressively constrained fIPAR maxima (0.86–0.90 and 0.72–0.78, respectively). These findings reinforce the conceptual understanding that fIPAR is tightly coupled to canopy structure and green-leaf duration (Norman & Welles, 1983; Monsi & Saeki, 2005; Chen *et al*., 2017). Similar magnitudes of IPAR reduction (20–35%) with delayed sowing have been documented in wheat and other cereals, where accelerated senescence shortens the effective radiation capture window despite comparable incident PAR (Borrelli, *et al*., 2011; Mubvuma *et al*., 2020).

Interannual differences in IPAR observed between Rabi 2020–21 and 2021–22 further emphasize the sensitivity of radiation interception to seasonal weather variability, particularly temperature and radiation regimes during vegetative and reproductive stages (Vashisth *et al*., 2022; Lollato *et al*., 2019). Slightly lower IPAR during 2021–22 coincided with higher temperatures and reduced canopy longevity, reinforcing earlier observations that warming shortens the duration of effective radiation interception even when early canopy development is adequate (Asseng *et al*., 2015; Chenu *et al*., 2013).

Biomass accumulation and its radiation basis

The strong correspondence between IPAR, fIPAR and biomass accumulation across sowing dates and seasons confirms that cumulative intercepted radiation is a primary determinant of dry matter production in wheat. Biomass reductions of 25–35% under very late sowing closely mirrored declines in IPAR and fIPAR, consistent with previous reports from the IGP and other heat-prone environments (Aggarwal & Mall, 2002; Pradhan *et al*., 2018; Dubey *et al*., 2021). Elevated terminal temperatures likely accelerated leaf senescence and reduced assimilatory capacity during grain filling, thereby limiting biomass accumulation despite adequate early-season growth (Aslam *et al*., 2025; Asseng *et al*., 2015).

Yield response and canopy–radiation linkages

Grain yield responses across both seasons closely tracked variations in canopy development, radiation interception and biomass production. Yield reductions of 6–10% under moderately delayed sowing and 22–29% under very late sowing is consistent with documented yield penalties associated with terminal heat stress and shortened grain-filling duration in wheat (Porter & Gawith, 1999; Lobell *et al*., 2012; Zhao *et al*., 2017). The alignment between yield losses and reductions in LAI, IPAR and biomass underscores that yield formation in wheat is strongly constrained by the duration and efficiency of canopy radiation capture rather than by sink limitation alone, as also reported by (Slafer *et al*. 2014).

Genotypic differences and adaptation to delayed sowing

Among the three cultivars, HD 3086 consistently exhibited superior canopy persistence, higher LAI, greater IPAR and fIPAR, and consequently higher biomass and yield stability under delayed sowing. This performance suggests enhanced tolerance to thermal stress, likely associated with delayed senescence, improved canopy architecture and sustained photosynthetic activity, traits previously identified as critical for wheat adaptation to warming environments (Reynolds *et al*., 2012; Sukumaran *et al*., 2018). The comparatively greater sensitivity of PBW 723 aligns with earlier studies showing that early-maturing cultivars often sacrifice canopy duration and radiation capture under stress, limiting biomass accumulation and yield potential (Prasad *et al*., 2017).

Implications for wheat management under climate variability

Collectively, these results reinforce that timely sowing remains the most effective agronomic strategy for maximizing canopy development, radiation interception and yield under the climatic conditions of the IGP. The clear mechanistic linkage between phenology, canopy radiation capture and productivity also suggests that breeding strategies targeting canopy persistence, delayed senescence and stable fIPAR under thermal stress will be essential for sustaining wheat yields under future warming scenarios (Reynolds *et al*., 2021; Asseng *et al*., 2020). Integrating such traits with optimized sowing windows can substantially enhance the resilience of wheat-based cropping systems in heat-prone environments.

Conclusions

The study highlights that weather variability, particularly temperature and radiation regimes associated with sowing time, exerts a decisive influence on canopy radiation interception and wheat yield. Timely sowing aligned crop phenology with favourable weather conditions, enhancing LAI development, sustaining higher fIPAR and cumulative IPAR, and thereby maximizing biomass accumulation and grain yield. In contrast, delayed sowing exposed the crop to adverse thermal conditions, shortened the duration of effective radiation interception, and caused substantial yield penalties. Genotypic differences in canopy stability moderated these effects, with HD 3086 demonstrating superior resilience under variable weather conditions. Overall, optimizing sowing time and selecting canopy-stable genotypes are critical for mitigating weather-induced yield variability in wheat.

Acknowledgements

This work is a part of the PhD research programme, and the financial support from ICAR-Indian Agricultural Research Institute (IARI) is gratefully acknowledged. The authors are thankful to the Director, IARI, New Delhi, and the Head of the Division of Agricultural Physics, IARI, New Delhi, for their encouragement and support during the study.

References

Aggarwal, P.K. and Mall, R.K. 2002. Climate change and rice yields in diverse agro-environments of India. I. Effect of temperatures. *Field Crops Research*, **80(2)**: 73–85. https://doi.org/10.1016/S0378-4290(02)00190-9

Aravind, K.S., Vashisth, A., Roy, D. and Krishnan, P. 2022. Multistage Wheat Yield Estimation using Biophysical Parameters under Different Weather Condition at Semi-arid Region of India. *Journal of Agricultural Physics*, **22(2)**: 131-141.

Aslam, I., Bilal, M., Tariq, F., Saeed, R.M.F., Fatima, S.A., Rizwan, M., Ahmad, M. and Bilal, M. 2025. Climate Change and Crop Productivity: A Global Review of Impacts, Adaptation, and Future Challenges. http://dx.doi.org/10.18782/2582-7146.253

Asseng, S., Ewert, F., Martre, P., Rötter, R.P., Lobell, D.B., Cammarano, D., Kimball, B.A., Ottman, M.J., Wall, G.W., White, J.W. and Reynolds, M.P. 2015. Rising temperatures reduce global wheat production. *Nature Climate Change*, **5**: 143–147. https://doi.org/10.1038/nclimate2470

Asseng, S., Guarin, J.R., Raman, M., Monje, O., Kiss, G., Despommier, D.D., Meggers, F.M. and Gauthier, P.P. 2020. Wheat yield potential in controlled-environment vertical farms. *Proceedings of the National Academy of Sciences*, **117**: 19131–19135. https://doi.org/10.1073/pnas.2002655117

Borrelli, G., Ficco, D., Giuzio, L., Pompa, M., Cattivelli, L. and Flagella, Z. 2011. Durum wheat salt tolerance in relation to physiological, yield and quality characters. *Cereal Research Communications*, **39(4)**: pp.525-534. https://doi.org/10.1556/crc.39.2011.4.7

Chen, J.M., Liu, J., Cihlar, J. and Goulden, M.L. 2017. Daily canopy photosynthesis model through temporal and spatial scaling for remote sensing applications. *Ecological Modelling*, **124**: 99–119.

Chenu, K., Deihimfard, R. and Chapman, S.C. 2013. Large-scale characterization of drought pattern: A continent-wide modelling approach applied to the Australian wheatbelt. *European Journal of Agronomy*, **82**: 36–52.

Dubey, R., Pathak, H., Chakrabarti, B., Singh, S., Gupta, D.K. and Harit, R.C. 2020. Impact of terminal heat stress on wheat yield in India and options for adaptation. *Agricultural Systems*, **181**: 102826. https://doi.org/10.1016/j.agsy.2020.102826

Joshi, A.K., Mishra, B., Chatrath, R., Ortiz Ferrara, G. and Singh, R.P. 2007. Wheat improvement in India: present status, emerging challenges and future prospects. *Euphytica*, **157(3)**: 431-446. https://doi.org/10.1007/s10681-007-9385-7

Lobell, D.B., Schlenker, W. and Costa-Roberts, J. 2012. Climate trends and global crop production since 1980. *Science*, **333**: 616–620. https://doi.org/10.1126/science.1204531

Lollato, R.P., Edwards, J.T. and Ochsner, T.E. 2017. Meteorological limits to winter wheat productivity in the US southern Great Plains. *Field Crops Research*, **203**: 212-226. https://doi.org/10.1016/j.fcr.2016.12.014

Monsi, M. and Saeki, T. 2005. On the factor light in plant communities and its importance for matter production. *Annals of Botany*, **95**: 549–567. (Original work published 1953)

Monteith, J.L. 1977. Climate and the efficiency of crop production in Britain. *Philosophical Transactions of the Royal Society B*, **281**: 277–294.

Mubvuma, M.T., Ogola, J.B. and Mhizha, T. 2021. Effect of planting date and genotype on intercepted radiation and radiation use efficiency in chickpea crop (*Cicer arietinum* L.). *Cogent Food & Agriculture*, **7(1)**: 1899422. https://doi.org/10.1080/23311932.2021.1899422

Norman, J.M. and Welles, J.M. 1983. Radiative transfer in an array of canopies. *Agronomy Journal*, **75**: 481–488. https://doi.org/10.2134/agronj1983.00021962007500030016x

Pathania, R., Prasad, R., Rana, R.S. and Mishra, S.K. 2019. Heat unit requirement and yield of wheat (*Triticum aestivum* L.) varieties under different growing environment in mid hill conditions of Himachal Pradesh. *Journal of Agrometeorology*, **21(3)**: 282-287.

Porter, J.R. and Gawith, M. 1999. Temperatures and the growth and development of wheat. *European Journal of Agronomy*, **10**: 23–36. https://doi.org/10.1016/S1161-0301(98)00047-1

Pradhan, S., Bandyopadhyay, K.K. and Joshi, D.K. 2012. Canopy reflectance spectra of wheat as related to crop yield, grain protein under different management practices. *Journal of Agrometeorology*, **14(1)**: 21-25. https://doi.org/10.54386/jam.v14i1.1373

Prasad, P.V., Pisipati, S.R., Ristic, Z., Bukovnik, U. and Fritz, A.K. 2008. Impact of nighttime temperature on physiology and growth of spring wheat. *Crop Science*, **48(6)**: 2372-2380. https://doi.org/10.2135/cropsci2007.12.0717

Reynolds, M.P., Ortiz-Monasterio, J.I. and McNab, A. 2012. Physiological breeding I: Interdisciplinary approaches to improve crop adaptation. CIMMYT. http://hdl.handle.net/10883/1287

Reynolds, M.P., Lewis, J.M., Ammar, K., Basnet, B.R., Crespo-Herrera, L., Crossa, J., Dhugga, K.S., Dreisigacker, S., Juliana, P., Karwat, H. and Kishii, M. 2021. Harnessing translational research in wheat for climate resilience. *Journal of Experimental Botany*, **72(14)**: 5134-5157. https://doi.org/10.1093/jxb/erab256

Debasish Roy, D., Vashisth, A., Krishnan, P., Mukherjee, J., Meena, M.C., Biswakarma, N., Rathore, P., Bag, K. and Kumari, S. 2024. Delayed sowing and its ramifications: biophysical, yield and quality analysis of wheat cultivars in the northwest Indo Gangetic plains. *Journal of the Science of Food and Agriculture*, **104(11)**: 6831-6843

Sandana, P., Ramírez, M. and Pinochet, D. 2012. Radiation interception and radiation use efficiency of wheat and pea under different P availabilities. *Field Crops Research*, **127**: 44-50. https://doi.org/10.1016/j.fcr.2011.11.005

Sinclair, T.R. and Muchow, R.C. 1999. Radiation use efficiency. *Advances in Agronomy*, **65**: 215–265. https://doi.org/10.1016/S0065-2113(08)60914-1

Slafer, G.A. and Rawson, H.M. 1994. Sensitivity of wheat phasic development to major environmental factors. *Field Crops Research*, **38**: 203–210. https://www.cabidigitallibrary.org/doi/full/10.5555/19940706911

Slafer, G.A., Savin, R. and Sadras, V.O. 2014. Coarse and fine regulation of wheat yield components. *Field Crops Research*, **158**: 71–83. https://doi.org/10.1016/j.fcr.2013.12.004

Sukumaran, S., Reynolds, M.P. and Sansaloni, C. 2018. Genome-wide association analyses identify loci for canopy temperature and yield under heat stress. *Theoretical and Applied Genetics*, **131**: 2151–2166. https://doi.org/10.3389/fpls.2018.00081

Sun, H., Shao, L., Chen, S., Wang, Y. and Zhang, X. 2013. Effects of sowing time and rate on crop growth and radiation use efficiency of winter wheat in the North China Plain. *International Journal of Plant Production*, **7(1)**: 117-137.

Vashisth, A., Goyal, A. and Krishanan P. 2020. Effect of weather variability on growth and yield of wheat crop under semi-arid region of India. *Journal of Agrometeorology*, **22 (2)**: 124-131.

Vashisth, A., Roy, D., Goyal A. and Krishanan P. 2022. Influence of meteorological parameters on wheat yield under different sowing conditions. *Mausam*, **73(1)**: 161-172.

Vashisth, A., Jain, A.K., Das, D.K., Joshi, D.K., Sharma, P.K. and Baloda, R. 2012. Effect of weather variability on growth characteristics and seed yield of Soybean crop. *Journal of Agrometeorology*, **14**: 100-106.

Yunusa, I.A.M., Siddique, K.H.M., Belford, R.K. and Karimi, M.M. 1993. Effect of canopy structure on efficiency of radiation interception and use in spring wheat cultivars during the pre-anthesis period in a Mediterranean-type environment. *Field Crops Research*, **35(2)**: 113-122. https://doi.org/10.1016/0378-4290(93)90144-C

Zhao, C., Liu, B., Piao, S., Wang, X., Lobell, D.B., Huang, Y., Huang, M., Yao, Y., Bassu, S., Ciais, P. and Durand, J.L. 2017. Temperature increase reduces global yields of major crops in four independent estimates. *Proceedings of the National Academy of Sciences*, **114(35)**: 9326-9331. https://doi.org/10.1073/pnas.1701762114

Received: 5 August 2025; Accepted: 15 October 2025